

Article

Effects of *Antheraea pernyi* on Parasitization of *Kriechbaumerella dendrolimi* by Using Immunology and Metabolomics

Yuwen Que ^{1,†}, Xinyuan Fang ^{1,†}, Zhenhui Zhao ¹, Zhenhong Chen ¹, Ciding Lu ¹, Qiufang Zheng ¹, Jiajin Tan ², Feiping Zhang ¹ and Guanghong Liang ^{1,*} 

¹ Forestry College, Fujian Agriculture and Forestry University, Fuzhou 350002, China; yw.que@fafu.edu.cn (Y.Q.); 1210429003@fafu.edu.cn (X.F.); 12304029010@fafu.edu.cn (Z.Z.); 12304029011@fafu.edu.cn (Z.C.); 2210429001@fafu.edu.cn (C.L.); 52304022043@fafu.edu.cn (Q.Z.); fpzhang@fafu.edu.cn (F.Z.)

² Forestry College, Nanjing Forestry University, Nanjing 210037, China; tanjiajin@njfu.edu.cn

* Correspondence: guanghong.liang@fafu.edu.cn

† These authors contributed equally to this work.

Abstract: *Kriechbaumerella dendrolimi* (Hymenoptera, Chalcididae) is a dominant pupal parasitoid species of various significant pine caterpillars, including *Dendrolimus houi* Lajonquiere (Lepidoptera, Lasiocampidae), with great potential for utilization. So far, the mass rearing of *K. dendrolimi* has been successfully established using *Antheraea pernyi* (Lepidoptera, Saturniidae) pupae as alternative hosts and released in the forest to suppress *D. houi* populations. However, the outcome is still expected to be improved due to lower parasitism rates, which might be related to the autonomous immune function of *A. pernyi* pupae. In our study, we investigated the effects of *K. dendrolimi* parasitization on the immune responses of *A. pernyi* pupae by measuring the expression of key immune factors: superoxide dismutase (SOD), polyphenol oxidases (PPOs), Attacin, Lysozymes (LYSs), and serine proteases (PRSSs). Our results show that parasitization significantly upregulated these immune factors, with distinct temporal patterns observable between 4 and 48 h post-parasitization. This upregulation highlights a robust immune response, adapting over time to the parasitic challenge. These findings suggest that specific immune mechanisms in *A. pernyi* pupae are activated in response to *K. dendrolimi*, shedding light on potential targets for enhancing host resistance. Metabolomic analyses complemented these findings by illustrating the broader metabolic shifts associated with the immune response. Specifically, Attacin was significantly upregulated twice, hypothesizing that the parasitoid's venom contains at least two parasitic factors. Metabolomics analysis revealed a significant metabolite difference within parasitized *A. pernyi* pupae. The highest number of differential expression metabolites (DEMs) was observed at 16 h post-parasitism (1184 metabolites), with fewer DEMs at 8 h (568 metabolites) and 32 h (693 metabolites), suggesting a close relationship between parasitism duration and the number of DEMs. These fluctuations reflected the fundamental process of immune interaction. KEGG enrichment results showed that the DEMs were mainly enriched in energy metabolism and immune-related pathways, indicating that parasitism is a process of continuous consumption and immune interaction in the host. These DEMs could also become future targets for regulating the immune functions of *A. pernyi* pupae and could provide reference data for optimizing mass-rearing techniques.

Keywords: *Antheraea pernyi*; *Kriechbaumerella dendrolimi* Sheng and Zhong; immune effects; immune factor; metabolomics analysis



Citation: Que, Y.; Fang, X.; Zhao, Z.; Chen, Z.; Lu, C.; Zheng, Q.; Tan, J.; Zhang, F.; Liang, G. Effects of *Antheraea pernyi* on Parasitization of *Kriechbaumerella dendrolimi* by Using Immunology and Metabolomics. *Forests* **2024**, *15*, 851. <https://doi.org/10.3390/f15050851>

Academic Editors: Daniela K. Pilarska, Margarita Georgieva and Georgi Georgiev

Received: 30 March 2024

Revised: 5 May 2024

Accepted: 8 May 2024

Published: 13 May 2024



Copyright: © 2024 by the authors. Licensee MDPI, Basel, Switzerland. This article is an open access article distributed under the terms and conditions of the Creative Commons Attribution (CC BY) license (<https://creativecommons.org/licenses/by/4.0/>).

1. Introduction

The *Dendrolimus houi* Lajonquiere (Lepidoptera, Lasiocampidae) is a major defoliator in the southern forest regions of China, often causing widespread dieback and severe economic and ecological losses from larvae feeding on needles and tender branches of pine

trees [1–5]. Previous research indicates that *Kriechbaumerella dendrolimi* Sheng and Zhong (Hymenoptera, Chalcididae), a parasitoid wasp, exhibits high natural parasitism rates, short life cycles, and high offspring production. It effectively controls *D. hou* [6,7] and is a crucial natural enemy of various Lepidopteran pests such as *D. punctatus* Walker and *D. kikuchii* Matsumura, thus holding great developmental potential [8,9]. In the artificial mass-rearing system of *K. dendrolimi*, *Antheraea pernyi* is the most suitable alternative host for mass rearing. However, the parasitism rate of *A. pernyi* pupae remains low [8], which is one of the main factors limiting the efficiency and cost of mass rearing. Based on the melanization phenomenon observed within the parasitized *A. pernyi* pupae, it is hypothesized that the low parasitism rate is related to the autonomous immune function of *A. pernyi* pupae.

Insects lack adaptive immunity but possess an efficient innate immune system capable of successfully defending against exogenous pathogenic infections [10]. The main forms of immunity are cellular and humoral [11,12]. Humoral immunity refers to immune reactions involving soluble effector molecules such as antimicrobial peptides (AMPs), complement-like proteins, and enzymes involved in melanin cascades [13,14]. When insects are attacked, serine proteases (PRSSs) initiate cascade reactions affecting the Toll pathway [15]. The AMPs, as vital effectors of insect humoral immunity, are subsequently controlled by pathways such as Toll and participate in eliminating foreign pathogens [16,17]. Moreover, Lysozymes (LYSs) are another type of lytic protein that could cleave the β -1,4 glycosidic linkages between N-acetylglucosamine and N-acetylmuramic acid in peptidoglycans, one component of the bacterial cell wall, activating melanin-based pathways and causing melanization [18–20]. Meanwhile, various enzymes and metabolites in insects, such as hemolymph proteins, polyphenol oxidases (PPOs), and superoxide dismutase (SOD), also respond rapidly and participate in defense reactions [21,22]. These immune factors play a crucial role in protecting insects from foreign biological invasions, and their changes can reveal the immune interaction process between the parasitoid and the host to some extent.

Furthermore, insect metabolic products play a crucial role in regulating their physiology, behavior, and adaptation [23], and changes in metabolic products can often be identified using metabolomics techniques [24]. Recently, these techniques have been widely applied to explore insect immune mechanisms [25,26]. Therefore, this study aims to reveal the immune mechanism of *A. pernyi* pupae against *K. dendrolimi* by measuring the expression of five immune factors: SOD, PPOs, Attacin, LYSs, and PRSSs before and after parasitism and combining metabolomic analyses. This will provide a theoretical basis for the mass rearing of *K. dendrolimi*.

2. Materials and Methods

2.1. Rearing of Test Insects and Sample Preparation

2.1.1. Rearing of Test Insects

The test parasitoids *K. dendrolimi* and fertilized eggs of *A. pernyi* were sourced from the indoor population at the Provincial Key Laboratory of Integrated Pest Management in Ecological Forests, Fujian Agriculture and Forestry University (26°05'06.0'' N 119°14'07.0'' E). *K. dendrolimi* was propagated indoors using *A. pernyi* pupae as hosts. The environmental conditions were meticulously controlled, maintaining a temperature of 24 ± 2 °C and a relative humidity of $60 \pm 10\%$. Upon emergence, the parasitoids were fed with 100% honey applied to rayon balls. A 1:1 male-to-female ratio was maintained for mating, allowing the parasitoids to mate freely within rearing boxes (14.1 cm \times 6.3 cm \times 8.5 cm) over a period of 24 h. Each rearing cage contained ten males and ten females. After this period, female wasps were selected as experimental insects [8]. After hatching, *A. pernyi* larvae were reared on *Quercus aliena* leaves under controlled conditions with a temperature of 24 ± 2 °C and relative humidity of $60 \pm 10\%$. The larvae were housed in specified rearing cages (40 cm \times 30 cm \times 40 cm) until they pupated. Post-pupation, the pupae were stored at 4 °C in a refrigerator for further use [8,27]. Pupae of *A. pernyi* that were healthy, active, and free of external injuries, all uniformly sized with a body length of 5 cm \pm 0.2 cm and a width of 2 cm \pm 0.1 cm, were then selected as the test hosts.

2.1.2. Collection of Hemolymph Samples from Host Insects

Parasitism was conducted in a one-to-one ratio of wasp to *A. pernyi* pupa. Hemolymph samples were collected from non-parasitized (CK) and parasitized *A. pernyi* pupae at intervals of 4 h from 4 to 48 h post-parasitism. The surface of each pupa was rinsed with sterile water, disinfected with 75% alcohol spray, and then allowed to air dry. The lower abdomen of each pupa was dissected with a sterile scalpel to collect the hemolymph into sterile centrifuge tubes [28,29]. The samples were immediately flash-frozen in liquid nitrogen for 15 min and then stored at -80°C for further analysis. Each sample consisted of hemolymph collected from six pupae.

2.2. Determination of Immune Factors in Host Insect Hemolymph

2.2.1. SOD Activity Assay

A $20\times$ concentrated wash buffer was prepared by diluting with distilled water. Hemolymph samples from *A. pernyi* pupae were allowed to clot at room temperature for 15 min, followed by centrifugation at 2000 rpm for 20 min to collect the supernatant. This extraction process was repeated twice to ensure consistency. Using the Insect SOD Assay Kit (YJ403841, Shanghai Enzyme-linked Biotechnology Co., Ltd., Shanghai, China), 50 μL of standards at concentrations of 200, 100, 50, 25, 12.5, and 0 U/mL were added sequentially to six standard wells. For each sample well, 40 μL of sample diluent and 10 μL of the sample were added, followed by gentle shaking to mix. Subsequently, 100 μL of the enzyme-label reagent was added to each well. The plate was covered with a sealing film and incubated in a 37°C water bath for 60 min. After incubation, the sealing film was removed, the liquid discarded, and the wells flicked dry. Each well was filled with wash buffer, left to stand for 30 s, and emptied. This washing step was repeated five times before flicking dry. Then, 50 μL of chromogen solution A and 50 μL of chromogen solution B were added to each well, gently shaken to mix, and incubated in the dark at 37°C for 15 min for color development. Finally, 50 μL of stop solution was added to each well, and each well's optical density (OD value) was sequentially measured at 450 nm wavelength using an ELISA reader (SpectraMax iD5, Molecular Devices, San Jose, CA, USA). Each sample was tested eight times, and the average value was taken. The standard curve's linear regression equation was calculated using the concentrations and OD values of the standards. The enzyme activity of the samples was calculated by substituting the sample OD values into the standard curve equation [30].

2.2.2. PPO Activity Assay

The insect PPO activity was measured using the Polyphenol Oxidase Assay Kit (YJ480715, Shanghai Enzyme-linked Biotechnology Co., Ltd., Shanghai, China). Except for adding standard solutions to six standard wells at concentrations of 2000, 1000, 500, 250, 125, and 0 U/mL, the other steps were consistent with Section 2.2.1.

2.2.3. Attacin Activity Assay

The activity of the insect Attacin was determined using the Attacin Assay Kit (YJ217054, Shanghai Enzyme-linked Biotechnology Co., Ltd., Shanghai, China). Except for adding standard solutions to six standard wells at concentrations of 800, 400, 200, 100, 50, and 0 pg/mL , the other steps were consistent with Section 2.2.1.

2.2.4. LYS Activity Assay

The activity of insect LYSs was measured using the Lysozyme Assay Kit (YJ409903, Shanghai Enzyme-linked Biotechnology Co., Ltd., Shanghai, China). Except for adding standard solutions to six standard wells at concentrations of 20, 10, 5, 2.5, 1.25, and 0 U/L, the other steps were consistent with Section 2.2.1.

2.2.5. PRSS Activity Assay

The activity of insect PRSSs was determined using the Serine Protease Assay Kit (YJ440300, Shanghai Enzyme-linked Biotechnology Co., Ltd., Shanghai, China). Except for adding standard solutions to six standard wells at concentrations of 64, 32, 16, 8, 4, and 0 U/L, the other steps were consistent with Section 2.2.1.

2.3. Sample Preparation for HPLC-Mass

Hemolymph samples from *A. pernyi* pupae were selected as metabolomic experiment samples at various stages: non-parasitized (CK), 8 h after parasitization (AP8h), 16 h after parasitization (AP16h), and 32 h after parasitization (AP32h). For each sample, 100 μ L was measured and mixed with 500 μ L of extraction solvent (methanol–acetonitrile–water, *v/v*, 2/2/1 with an internal standard concentration of 2 mg/L) at a ratio of 1000:2. The mixture was vortexed for 30 s and ultrasonicated for 10 min in an ice-water bath. After ultrasonication, the samples were left to stand at -20 °C for 1 h and then centrifuged at 4 °C for 15 min at 12,000 rpm. Subsequently, 500 μ L of the supernatant was transferred into an Eppendorf tube and dried in a vacuum concentrator. The dried metabolites were then reconstituted with 160 μ L of acetonitrile–water (*v/v*, 1/1), vortexed for 30 s, ultrasonicated in an ice-water bath for 10 min, and finally centrifuged at 4 °C for 15 min at 12,000 rpm. After this, 120 μ L of the supernatant was transferred to a sample vial for analysis [31]. Each sample was analyzed with a 10 μ L injection volume.

2.4. Metabolite Profiling

Metabolomic analysis was performed using a liquid–mass system consisting of an ultra-high-performance liquid phase (Waters Acquity I-Class PLUS, Waters, Framingham, MA, USA) tandem high-resolution mass spectrometer (Waters Xevo G2-XS QToF, Waters, Framingham, MA, USA). The column model used was an AcquityUPLC HSS T3 column (1.8 μ m \times 2.1 mm \times 100 mm). The liquid phase separation condition was mobile phase A (0.1% formic acid aqueous solution) and mobile phase B (0.1% formic acid acetonitrile) gradient elution [32]. The elution process started with 2% mobile phase B and was maintained for 0.25 min. The mobile phase B increased uniformly from 0.25 to 10 min to 98% and maintained for 3 min. It was then returned to the initial condition of 2% mobile phase B and held for 2 min, then was analyzed in the next sample. The flow rate was 0.4 mL/min, and the sample volume was 1 μ L. The mass spectrometer detection conditions were as follows: capillary voltage: 2000 V (positive ion modes) or -1500 V (negative ion modes), cone hole voltage: 30 V, ion source temperature: 150 °C, desolvation temperature: 500 °C, flow rate of back blowing: 50 L/h, and desolvent gas flow rate: 800 L/h [33].

2.5. Qualitative and Quantitative Analyses of Metabolites

The metabolites were identified and quantified based on the online METLIN database of Progenesis QI software (v3.0) and the self-built database of Beijing BioMaker Technologies Co. (Beijing, China). Theoretical fragmentation identification was also conducted with a parent ion mass deviation within 100 ppm and fragment ion mass deviation within 50 ppm. R software (v4.1.3, <https://www.r-project.org/>, accessed on 5 May 2023) was employed for principal component analysis (PCA) [34]. An OPLS-DA (orthogonal partial least squares discriminant analysis) model was employed with the first principal component of VIP (variable importance in the projection) ≥ 1 , combined with Student's *t*-test ($p < 0.05$) and FC (fold change) > 1.5 , to identify the differential expression metabolites (DEMs) [35]. Additionally, the DEMs were functionally annotated, and metabolic pathway enrichment analysis was performed using the Kyoto Encyclopedia of Genes and Genomes (KEGG) database [36].

2.6. Enzymatic Activity Data Analysis

Experimental results are presented as mean \pm standard deviation (SD). Data were analyzed using SPSS 25.0 software. After testing for normal distribution and homogeneity

of variances, statistical analyses were conducted using Fisher's LSD for group comparisons [37]. A p -value of less than 0.05 was considered statistically significant.

3. Results

3.1. Impact of *K. dendrolimi* Parasitization on the Hemolymph Immune Factors of *A. pernyi* Pupae

After parasitization by *K. dendrolimi*, the activity of five immune factors in *A. pernyi* pupae was significantly higher than in the control, indicating that the parasitism activated the host's immune response and enhanced its immunity level. Specifically, the activity of SOD showed a clear upward trend starting from AP8h. It was significantly higher than CK ($p < 0.05$) from AP12h (12 h after parasitization), with more minor fluctuations after that (Figure 1a). The activity of PPOs gradually increased from the onset of parasitism, becoming significantly higher than CK from AP16h ($p < 0.05$) and then stabilizing, reaching a peak at AP32h (Figure 1b). The activity of Attacin significantly increased at AP4h (4 h after parasitization) and AP20h (20 h after parasitization) ($p < 0.05$), subsequently maintaining stability (Figure 1c). Within 48 h of parasitism, the LYS activity in the *A. pernyi* pupae was significantly higher than CK ($p < 0.05$), with the highest activity at AP32h, then beginning to decline (Figure 1d). PRSSs showed some increase before AP16h but did not reach significance ($p > 0.05$); it became significantly higher than CK from AP20h ($p < 0.05$) and reached its peak at AP32h, followed by a decrease (Figure 1e).

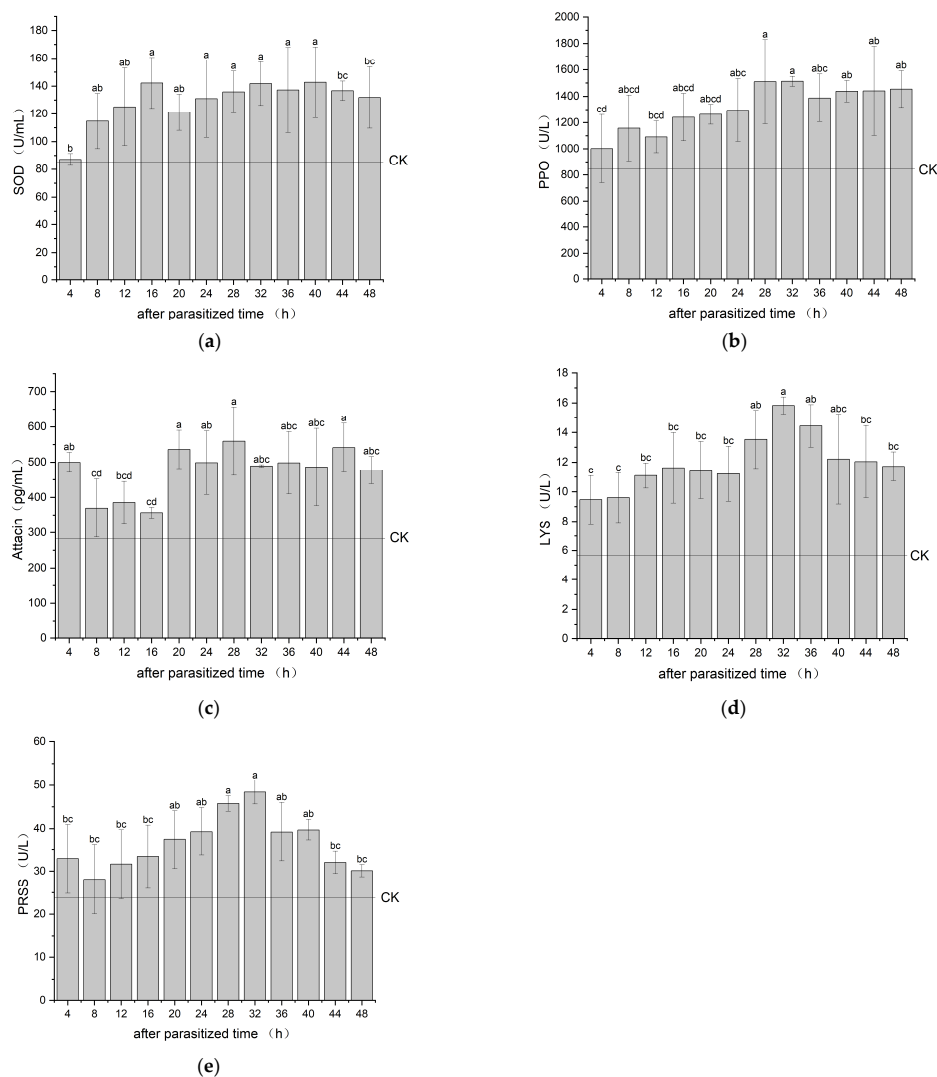


Figure 1. Changes in immune factors of *A. pernyi* pupae after parasitization by *K. dendrolimi*. (a) SOD activity in *A. pernyi* pupae after parasitization by *K. dendrolimi*; (b) PPO activity in *A. pernyi* pupae

after parasitization by *K. dendrolimi*; (c) Attacin activity in *A. pernyi* pupae after parasitization by *K. dendrolimi*; (d) LYS activity in *A. pernyi* pupae after parasitization by *K. dendrolimi*; (e) PRSS activity in *A. pernyi* pupae after parasitization by *K. dendrolimi*. Note: different lowercase letters indicate significant differences ($p < 0.05$).

Overall, AP8h and AP16h are critical turning points when early- to mid-stage immune factors change significantly, indicating that the immune response of *A. pernyi* entered a new phase. At the same time, AP32h is the peak point for multiple immune factors such as PPOs and LYSs, indicating the highest level of immune response of *A. pernyi* pupae to the parasitoid. These nodes reflect the physiological response time differences of the host at different stages to the parasitoid. Interestingly, the activity of Attacin significantly increased at AP4h but then decreased to levels similar to the control during the subsequent period (8–16 h) before significantly increasing again, indicating two stress responses in the Attacin during the immune process. This suggests that the venom of *K. dendrolimi* might contain multiple parasitic factors.

3.2. Impact of *K. dendrolimi* on the Hemolymph Metabolites of *A. pernyi* Pupae

The results of PCA analysis indicated that PC1 and PC2 accounted for 28.46% and 18.29% of the variation between different treatment groups, respectively (Figure 2). The samples parasitized by *K. dendrolimi* were distant from the CK group, suggesting significant differences in metabolite expression induced by parasitism in *A. pernyi* pupae.

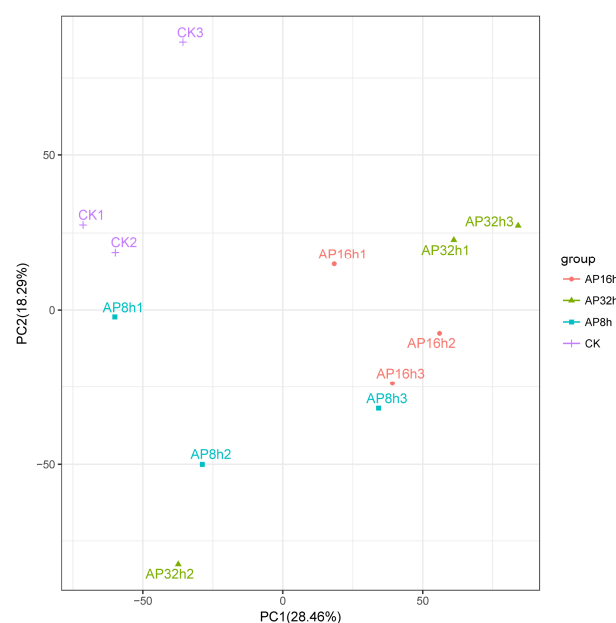


Figure 2. Score of PCA of metabolites of *A. pernyi*. Note: pupae non-parasitized (CK), 8 h after parasitization (AP8h), 16 h after parasitization (AP16h), and 32 h after parasitization (AP32h).

In OPLS-DA analysis, the CK-AP8h model explained 63.7% of the variance for the predictor variable X and 99.7% for the response variable Y and had a predictive ability of 80.5% for the sample variables (Figure 3a). The CK-AP16h model explained 64% of the variance for X and 100% for Y and had a predictive ability of 87.9% for the sample variables (Figure 3b). The CK-AP32h model explained 69.1% of the variance for X and 99.9% for Y and had a predictive ability of 89.5% for the sample variables (Figure 3c). The R2Y values in all three comparison combinations were close to 1, and the Q2Y values were all greater than 0.5, indicating suitable data quality and effective models suitable for subsequent analysis.

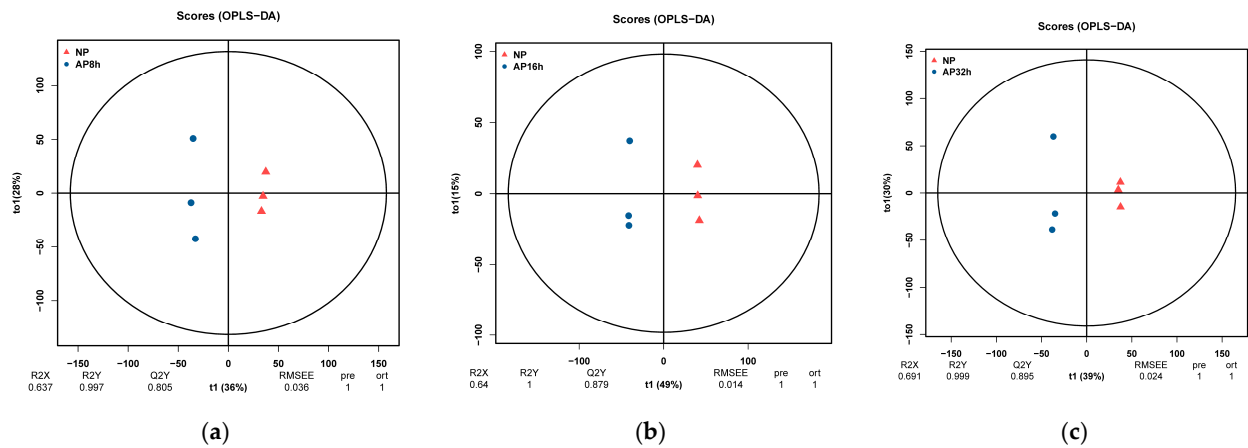


Figure 3. (a) Score of orthogonal projections to OPLS-DA score chart of CK-AP8h; (b) score of orthogonal projections to OPLS-DA score chart of CK-AP16h; (c) score of orthogonal projections to OPLS-DA score chart of CK-AP32h.

Analysis of the number of DEMs revealed that 568 DEMs were produced at AP8h compared to CK, with 268 upregulated and 300 downregulated. The notably upregulated DEMs included 2-Hydroxybutyric acid and 2-(L-Menthoxyl) ethanol, while significantly downregulated ones included 2-Oxoarginine and Uridine triphosphate (Figure 4a). At AP16h compared to CK, 1184 DEMs were identified, with 748 upregulated and 436 downregulated. Notable upregulated DEMs included Prolyl-Histidine, Cyanidin-3-o-beta-glucopyranoside, and (2S,4S)-Monatin, while significantly downregulated ones included Hexadecadienyl-carnitine (Figure 4b). At AP32h compared to CK, 693 DEMs were identified, with 293 upregulated and 400 downregulated. Notably, upregulated DEMs included 2'-Deamino-2'-hydroxyparamamine and 4'-Hydroxy-5,6,7,8-tetramethoxyflavone, while significantly downregulated ones included Pyrrolysine and Ureidoacrylate (Figure 4c). These DEMs might play an essential role in the immune process of *A. pernyi* pupae against the parasitoid. The number of DEMs was highest at AP16h. It decreased at AP32h, approaching the levels at AP8h, indicating significant differences in the immune response of *A. pernyi* pupae to parasitism by *K. dendrolimi* at different times, with the immune reaction being most intense at AP16h.

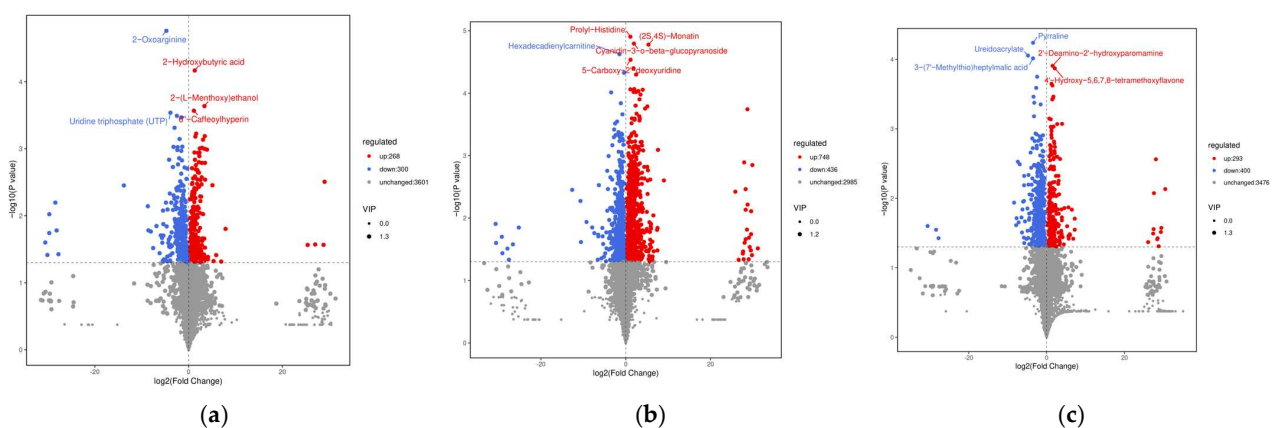
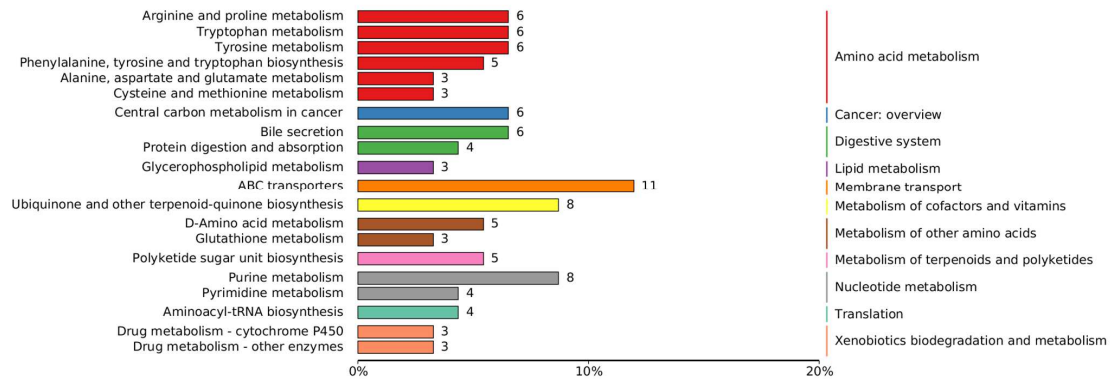
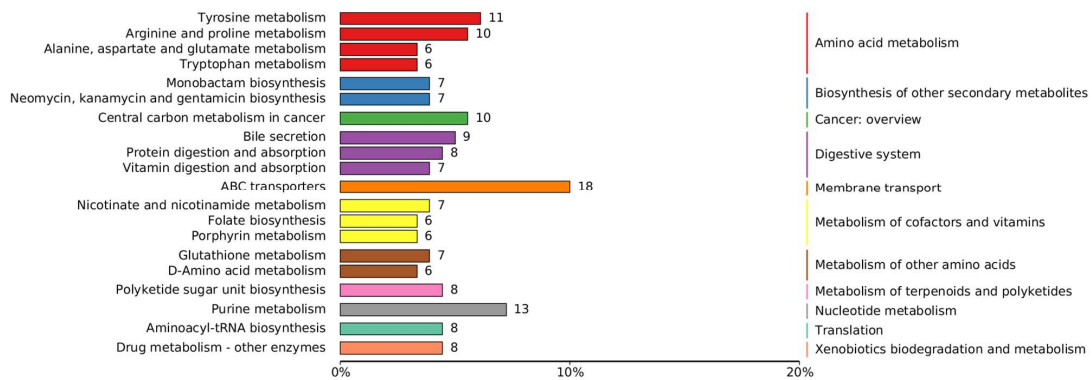


Figure 4. (a) Volcano plots of DEMs of CK-AP8h; (b) volcano plots of DEMs of CK-AP16h; (c) volcano plots of DEMs of CK-AP32h. Note: In the volcano plot, each point represents a metabolite. The *x*-axis represents the fold change of each substance in the comparison group (logarithm base 2); the *y*-axis represents the *p*-value from the *t*-test (logarithm base 10); the size of the dot indicates the variable importance in the projection (VIP) value from the OPLS-DA model. Blue dots represent downregulated DEMs; red dots represent upregulated DEMs; gray describes detected but not significant DEMs.

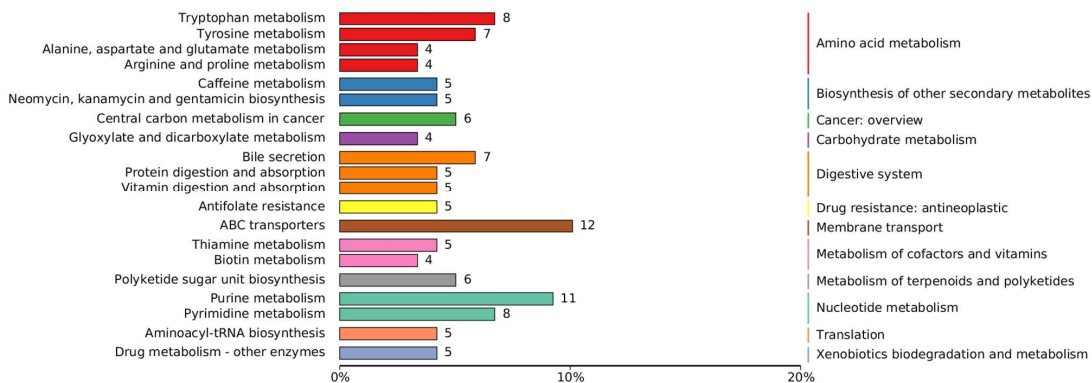
KEGG enrichment results showed that the DEMs produced at AP8h compared to CK were mainly enriched in amino acid metabolism (29), followed by nucleotide metabolism (12) and membrane transport (11) (Figure 5a). At AP16h compared to CK, the DEMs were also primarily enriched in amino acid metabolism (33), followed by the digestive system (24) and metabolism of cofactors and vitamins (20) (Figure 5b). At AP32h compared to CK, the DEMs were mainly enriched in amino acid metabolism (23), followed by nucleotide metabolism (19) and digestive system (10) (Figure 5c). These metabolic changes in these pathways might be related to the immune process. The consistent enrichment of amino acid metabolic pathways in all three periods indicates that parasitism by the *K. dendrolimi* has a sustained and significant impact on the amino acid metabolism of *A. pernyi* pupae.



(a)



(b)



(c)

Figure 5. (a) KEGG enrichment analysis of DEMs between CK and AP8h; (b) KEGG enrichment analysis of DEMs between CK and AP16h; (c) KEGG enrichment analysis of DEMs between CK and AP32h. Note: The numbers in the figure represent the quantities of DEMs.

4. Discussion

Previous research indicated that rapid and efficient immune responses were triggered to antagonize parasitic invasions within insects [38–41], characterized by swift activation of immune factors engaged in immune resistance activities such as metabolism of toxic substances [42–44], encapsulation of external pathogens [45,46], hemolymph agglutination [47], and wound healing processes [48]. Our study also revealed that upon parasitism, *A. pernyi* pupae show a significant increase in various immune factors from their hemolymph, indicating an intense immune response to the parasitization by *K. dendrolimi*. Among the immune effectors within insects, the AMPs played a dominant role, primarily by hydrolyzing bacterial cell walls and cell membrane permeability, inhibiting microbial division, and neutralizing metabolic toxins [49,50]. These peptides effectively disinfect bacteria, fungi, viruses, protozoa, and cancer cells [51–54]. We observed a rapid increase in the activity of Attacin, a major group of insect AMPs, within 4 h of parasitism by *K. dendrolimi*, followed by a rapid decrease between 8 and 16 h, before maintaining a consistently higher level [55–58], indicating at least two parasitic factors from the venom of *K. dendrolimi*, producing two times of intense change due to different response reactions from the immune system of *A. pernyi* pupae.

The innate immunity of host insects is critical to detect and eliminate external parasites, encompassing complex physiological, biochemical, and genetic interactions [38,40,59]. However, the metabolic adaptation to external invasions is another key factor influencing immune functions [60–62]. Following parasitism by *K. dendrolimi*, significant metabolic changes in *A. pernyi* pupae led to the production of specific DEMs directly related to insect immunity. For instance, 2-Hydroxybutyric acid, a biomarker linked to impaired cellular function and increased oxidative stress, participates in intracellular lipid oxidation and oxidative stress [63,64]. Furthermore, metabolites like 2'-Deamino-2'-hydroxypropylamine and Cyanidin-3-o-beta-glucopyranoside, involved in antibiotic biosynthesis and antioxidative activities, respectively [65–68], played a vital role in the immune process of *A. pernyi* pupae against *K. dendrolimi*. Additionally, the significant upregulation of 4'-Hydroxy-5,6,7,8-tetramethoxyflavone, known for its strong antiviral activity [69], at 32 h post-parasitism suggested the presence of viral elements in *K. dendrolimi*'s parasitic factors, regulating the host immune process.

KEGG enrichment analysis revealed that the DEMs produced in *A. pernyi* pupae post-parasitism mainly focused on pathways such as amino acid metabolism, nucleotide metabolism, membrane transport, and cofactors and vitamins metabolism, all closely related to energy metabolism [70,71]. Similar to the response of *Drosophila melanogaster* to microbial infections, the activation of immune functions in *A. pernyi* pupae increased the body's energy metabolic rate, with the additional energy consumption closely related to the synthesis of immune factors like AMPs [72–76]. Changes in membrane transport pathways affected energy metabolism and directly or indirectly influenced immune functions, such as nutrient intake, waste degradation and excretion, hormone release, and cell signaling [77,78]. Numerous studies indicate that key metabolites produced in hosts due to parasitization by parasitoid wasps can significantly affect the survival and reproduction of the parasitoids [79–81]. For instance, in their study, Liu et al. utilized metabolomics analysis to identify key metabolites, including lipids and amino acids, which can reduce the immune response of *Drosophila* hosts. Certain specific lipids and amino acids, such as L-histidine, L-proline, and L-glutamate, were crucial in this process [82]. These pathway alterations reflected the host insect's metabolic adaptation to parasitization. In summary, significant immune reactions and immune metabolites generated in parasitized *A. pernyi* pupae by *K. dendrolimi* may rapidly neutralize or resolve the parasitoid eggs during the early stages of parasitization, leading to lower parasitism. Therefore, the synthesis of these substances could be targeted for molecular modifications aimed at enhancing the reproductive efficiency of *K. dendrolimi*.

5. Conclusions

In the artificial rearing of *K. dendrolimi*, the alternative host *A. pernyi* pupae exhibited significant immune responses upon parasitism, specifically manifested as short-term significant upregulation of various immune factors and the DEMs related to energy metabolism and immune function. These are the primary causes of the lower parasitism rate of *K. dendrolimi*. The synthesis of these substances may serve as a molecular modification target to enhance the mass-rearing efficiency of *K. dendrolimi*.

Author Contributions: Conceptualization, Y.Q., X.F., C.L., Z.Z. and G.L.; data curation, Y.Q., X.F., Z.Z. and Q.Z.; investigation, Y.Q., X.F., Z.C. and C.L.; writing—original draft preparation, Y.Q., X.F., Z.C., Q.Z., J.T. and G.L., writing—review and editing, Y.Q., C.L., X.F., Z.Z., J.T., F.Z. and G.L. All authors have read and agreed to the published version of the manuscript.

Funding: This research was funded by the introductory project of the Fujian Provincial Science and Technology Department (No. 2021N002), the Fuzhou Forestry Science and Technology Research Project (No. 2021FZLY01), the Forestry Science and Technology Research Project of Fuzhou City (No. 2022-81), the Fujian Province Forestry Science and Technology Promotion Project (No. 2023TG16), the National Natural Science Fund of China (No. 31870641).

Data Availability Statement: The data presented in this study are available on request from the corresponding author.

Acknowledgments: In this study, we extend our gratitude to the Provincial Key Laboratory of Integrated Pest Management in Ecological Forests, Fujian Agriculture and Forestry University for providing the insect sources and experimental platform. We also thank the Forestry Bureau of Xiapu County and Minqing State-owned Forest Farm for their assistance in field collection and investigation.

Conflicts of Interest: The authors declare no conflicts of interest.

References

- Hai-yan, S.; Yun, L.; Zheng-hao, C.; Yin, H.; Chang-liang, L.; Zhu-he, Z.; Huai-feng, W.; Biao, H.; Fei-ping, Z.; Guang-hong, L. Effects of different host plants on the growth, reproduction and physiological enzyme activity of *Dendrolimus houi* Lajonquiere (Lepidoptera: Lasiocampidae). *For. Sci. Res.* **2022**, *35*, 63–70.
- Han, X.; Lu, C.; Geib, S.M.; Zheng, J.; Wu, S.; Zhang, F.; Liang, G. Characterization of *Dendrolimus houi* Lajonquiere (Lepidoptera: Lasiocampidae) transcriptome across all life stages. *Insects* **2019**, *10*, 442. [CrossRef] [PubMed]
- Xu, G.L. Research Advances on *Dendrolimus houi* in Yunnan Province. *J. Southwest For. Coll.* **2008**, *28*, 42–44.
- Liu, X. Study on biological characteristics and its integrated control of *Dendrolimus latipennis*. *J. Southwest For. Coll.* **2006**, *26*, 52–54.
- Bi, Z. Major Pest Control of *Pinus yunnanensis* in Yunnan. *Shaanxi For. Sci. Technol.* **2014**, *3*, 111–114.
- Lin, H.; Fu, L.; Lin, J.; Hua, Y.; Han, X.; Zheng, J.; He, H.; Zhang, F.; Liang, G. Main species of parasitic natural enemy insects within *Dendrolimus houi* (Lajonquiere) in the forest of *Cryptomeria fortunei* (Hooibrenk). *Chin. J. Biol. Control* **2017**, *33*, 842–848.
- Ting, J. Preliminary study on *Kriechbaumerella dendrolimi* Sheng and Zhong. *Jiangxi For. Sci. Technol.* **1993**, *5*, 19–20.
- Zheng, L.; Tang, J.; Chen, Z. Selectivity and Fitness of *Kriechbaumerella dendrolimi* to Different Forest Hosts. *Chin. J. Biol. Control* **2023**. Available online: <https://kns.cnki.net/kcms/detail/11.5973.S.20230706.1516.003.html> (accessed on 29 March 2024).
- Lin, H.Y.; Lu, C.D.; Chen, Z.H.; Zhou, Y.J.; Liang, Y.; Chen, H.; Liang, G.H. A survey on pupae parasitoid species of *Dendrolimus houi* (Lajonquiere) (Lepidoptera, Lasiocampidae) in China. *Biodivers Data J.* **2023**, *11*, e97878. [CrossRef]
- Rizki, T.M.; Rizki, R.M. The cellular defense system of *Drosophila melanogaster*. *Insect Ultrastruct.* **1984**, *2*, 579–604.
- Dunn, P.E. Humoral immunity in insects. *BioScience* **1990**, *40*, 738–744. [CrossRef]
- Lackie, A. Immune mechanisms in insects. *Parasitol. Today* **1988**, *4*, 98–105. [CrossRef] [PubMed]
- Blandin, S.; Levashina, E.A. Thioester-containing proteins and insect immunity. *Mol. Immunol.* **2004**, *40*, 903–908. [CrossRef] [PubMed]
- Imler, J.-L.; Bulet, P. Antimicrobial peptides in *Drosophila*: Structures, activities and gene regulation. *Mech. Epithel. Def.* **2005**, *86*, 1–21.
- Hillyer, J.F. Insect immunology and hematopoiesis. *Dev. Comp. Immunol.* **2016**, *58*, 102–118. [CrossRef] [PubMed]
- Liao, W.Y.; Lü, Z.H.; Zhang, Y.J.; Yang, Z.X. Insect humoral immune system, a new direction in the research of Bt resistance mechanisms in insect pests. *Acta Entomol. Sin.* **2022**, *65*, 1547–1564.
- Feng, S.; Tian, B.; Sun, Y.; Li, X.; Mi, R.; Wen, Z.; Meng, L.; Li, Y.; Li, S.; Du, X. Effect of Tussah Immunoreactive Substances and Tussah Antibacterial Peptide on Growth and Immunity of Yesso Scallop *Patinopecten yessoensis*. *Fish. Sci.* **2023**, *42*, 878–883.
- Mohamed, A.A.; Elmogy, M.; Dorrah, M.A.; Yousef, H.A.; Bassal, T. Antibacterial activity of lysozyme in the desert locust, *Schistocerca gregaria* (Orthoptera: Acrididae). *Eur. J. Entomol.* **2013**, *110*, 559–565. [CrossRef]

19. Ning, Y.X.; Su, Y.H.; Yang, M. cDNA cloning of lysozyme Pxllys of *Plutella xylostella* (Lepidoptera: Plutellidae) and the analysis of antibacterial activity of its recombinant protein. *Acta Entomol. Sin.* **2021**, *64*, 781–789.
20. Chapelle, M.; Girard, P.-A.; Cousserans, F.; Volkoff, N.-A.; Duvic, B. Lysozymes and lysozyme-like proteins from the fall armyworm, *Spodoptera frugiperda*. *Mol. Immunol.* **2009**, *47*, 261–269. [[CrossRef](#)]
21. Fu, Y.; Ma, Y.; Ren, S. Changes in physiological indices of *Antheraea pernyi* (Lepidoptera: Saturniidae) pupae induced by gram-positive bacteria *Bacillus thuringiensis* and gram-negative bacteria *Escherichia Coli*. *Acta Entomol. Sin.* **2016**, *59*, 192–199.
22. Chai, J.; Xie, D.; Tian, X.; Ran, R. Study on defense reactions of silkworm, *Bombyx mori* to *Cordyceps militaris*. *Southwest China J. Agric. Sci.* **2010**, *23*, 1308–1313.
23. Li, Z.; Cheng, Y.; Chen, J.; Xu, W.; Ma, W.; Li, S.; Du, E. Widely Targeted HPLC-MS/MS Metabolomics Analysis Reveals Natural Metabolic Insights in Insects. *Metabolites* **2023**, *13*, 735. [[CrossRef](#)] [[PubMed](#)]
24. Li, M.; Zhang, J.; Qin, Q.; Zhang, H.; Li, X.; Wang, H.; Meng, Q. Transcriptome and Metabolome Analyses of *Thitarodes xiaojinensis* in Response to *Ophiocordyceps sinensis* Infection. *Microorganisms* **2023**, *11*, 2361. [[CrossRef](#)] [[PubMed](#)]
25. Xu, Y.-J.; Luo, F.; Gao, Q.; Shang, Y.; Wang, C. Metabolomics reveals insect metabolic responses associated with fungal infection. *Anal. Bioanal. Chem.* **2015**, *407*, 4815–4821. [[CrossRef](#)]
26. Yang, S.; Zhang, H.; Jin, X. Determination of trimethyl phosphate of dichlorvos metabolite in tussah silkworm larvae by LC-MS/MS and analysis of its metabolic process. *Agrochemicals* **2023**, *7*, 504–509.
27. Zhang, Y.; Wang, F.; Zhao, Z. Metabonomics reveals that entomopathogenic nematodes mediate tryptophan metabolites that kill host insects. *Front. Microbiol.* **2022**, *13*, 1042145. [[CrossRef](#)]
28. Chan, Q.W.; Howes, C.G.; Foster, L.J. Quantitative Comparison of Caste Differences in Honeybee Hemolymph* S. *Mol. Cell. Proteom.* **2006**, *5*, 2252–2262. [[CrossRef](#)] [[PubMed](#)]
29. Łoś, A.; Strachecka, A. Fast and cost-effective biochemical spectrophotometric analysis of solution of insect “blood” and body surface elution. *Sensors* **2018**, *18*, 1494. [[CrossRef](#)]
30. Wang, X.; Zhang, X.; Zhang, X.; Liu, Q.; Zhang, X. Effect of azadirachtin on the hemocytes of *Oxya chinensis*. *Chin. J. Appl. Entomol.* **2019**, *56*, 546–556.
31. Zhu, Y.; Gao, H.; Han, S.; Li, J.; Wen, Q.; Dong, B. Antidiabetic activity and metabolite profiles of ascidian *Halocynthia roretzi*. *J. Funct. Foods* **2022**, *93*, 105095. [[CrossRef](#)]
32. Li, S.-L.; Song, J.-Z.; Choi, F.F.; Qiao, C.-F.; Zhou, Y.; Han, Q.-B.; Xu, H.-X. Chemical profiling of Radix Paeoniae evaluated by ultra-performance liquid chromatography/photo-diode-array/quadrupole time-of-flight mass spectrometry. *J. Pharm. Biomed. Anal.* **2009**, *49*, 253–266. [[CrossRef](#)]
33. Fang, X.; Chen, Z.; Chen, Z.; Chen, J.; Zhao, Z.; Wu, P.; Wu, H.; Zhang, F.; Liang, G. Metabolome and Transcriptome Analysis Reveals the Effects of Host Shift on *Dendrolimus houi* Lajonquière Larvae. *Forests* **2023**, *14*, 1307. [[CrossRef](#)]
34. Rong, W.T.; Song, Z.; Xin, L.; Deng, W.A.; Qin, Y.Y.; Li, X.D. Effects of combined pollution of heavy metals on the metabolomics of *Eucriotettix oculatus* (Orthoptera: Tetrigidae). *Acta Entomol. Sin.* **2022**, *65*, 437–450.
35. Bocca, C.; Kane, M.S.; Veyrat-Durebex, C.; Chupin, S.; Alban, J.; Kouassi Nzougnet, J.; Le Mao, M.; Chao de la Barca, J.M.; Amati-Bonneau, P.; Bonneau, D. The metabolomic bioenergetic signature of Opa1-disrupted mouse embryonic fibroblasts highlights aspartate deficiency. *Sci. Rep.* **2018**, *8*, 11528. [[CrossRef](#)] [[PubMed](#)]
36. Kanehisa, M.; Goto, S. KEGG: Kyoto encyclopedia of genes and genomes. *Nucleic Acids Res.* **2000**, *28*, 27–30. [[CrossRef](#)]
37. Williams, L.J.; Abdi, H. Fisher’s least significant difference (LSD) test. *Encycl. Res. Des.* **2010**, *218*, 840–853.
38. Carton, Y.; Poirié, M.; Nappi, A.J. Insect immune resistance to parasitoids. *Insect Sci.* **2008**, *15*, 67–87. [[CrossRef](#)]
39. Sato, R. Mechanisms and roles of the first stage of nodule formation in lepidopteran insects. *J. Insect Sci.* **2023**, *23*, 3. [[CrossRef](#)]
40. Castillo, J.C.; Reynolds, S.E.; Eleftherianos, I. Insect immune responses to nematode parasites. *Trends Parasitol.* **2011**, *27*, 537–547. [[CrossRef](#)]
41. Richman, A.; Kafatos, F.C. Immunity to eukaryotic parasites in vector insects. *Curr. Opin. Immunol.* **1996**, *8*, 14–19. [[CrossRef](#)] [[PubMed](#)]
42. Lynch, M.; Kuramitsu, H. Expression and role of superoxide dismutases (SOD) in pathogenic bacteria. *Microbes Infect.* **2000**, *2*, 1245–1255. [[CrossRef](#)]
43. Liu, N.Y.; Huang, J.M.; Ren, X.M.; Xu, Z.W.; Yan, N.S.; Zhu, J.Y. Superoxide dismutase from venom of the ectoparasitoid *Scleroderma guani* inhibits melanization of hemolymph. *Arch. Insect Biochem. Physiol.* **2018**, *99*, e21503. [[CrossRef](#)] [[PubMed](#)]
44. Colinet, D.; Cazes, D.; Belghazi, M.; Gatti, J.L.; Poirie, M. Extracellular superoxide dismutase in insects: Characterization, function, and interspecific variation in parasitoid wasp venom. *J Biol Chem* **2011**, *286*, 40110–40121. [[CrossRef](#)] [[PubMed](#)]
45. Bulet, P.; Charlet, M.; Hetru, C. Antimicrobial peptides in insect immunity. In *Innate immunity*; Springer: Berlin/Heidelberg, Germany, 2003; pp. 89–107.
46. Whitaker, J.R. Polyphenol oxidase. In *Food Enzymes: Structure and Mechanism*; Springer: Berlin/Heidelberg, Germany, 1995; pp. 271–307.
47. Gorman, M.J.; Paskewitz, S.M. Serine proteases as mediators of mosquito immune responses. *Insect Biochem. Mol. Biol.* **2001**, *31*, 257–262. [[CrossRef](#)] [[PubMed](#)]
48. Hedstrom, L. Serine protease mechanism and specificity. *Chem. Rev.* **2002**, *102*, 4501–4524. [[CrossRef](#)]
49. Zhang, M.; Chu, Y.; Zhao, Z.; An, C. Progress in the molecular mechanisms of the innate immune responses in insects. *Acta Entomol. Sin.* **2012**, *55*, 1221–1229.

50. Zhang, Q.; Li, K.; Wang, H. Research Progress of Antimicrobial Peptides from Black Soldier Fly. *Acta Agric. Univ. Jiangxiensis* **2022**, *4*, 996–1004.
51. Reddy, K.; Yedery, R.; Aranha, C. Antimicrobial peptides: Premises and promises. *Int. J. Antimicrob. Agents* **2004**, *24*, 536–547. [[CrossRef](#)]
52. Duan, X.; Li, H.; Zhang, R.; Wang, X. Progress of insect antimicrobial peptides. *J. Shenyang Pharm. Univ.* **2023**, *40*, 1401–1408.
53. Brady, D.; Grapputo, A.; Romoli, O.; Sandrelli, F. Insect cecropins, antimicrobial peptides with potential therapeutic applications. *Int. J. Mol. Sci.* **2019**, *20*, 5862. [[CrossRef](#)] [[PubMed](#)]
54. Xu, P.; Lv, D.; Guo, X. Advances in Inhibitory Effects of Insect Antimicrobial Peptides on Tumor Cells *Genom. Appl. Biol.* **2021**, *40*, 923–928.
55. Buonocore, F.; Fausto, A.M.; Della Pelle, G.; Roncevic, T.; Gerdol, M.; Picchiatti, S. Attacins: A promising class of insect antimicrobial peptides. *Antibiotics* **2021**, *10*, 212. [[CrossRef](#)] [[PubMed](#)]
56. Hultmark, D.; Engström, A.; Andersson, K.; Steiner, H.; Bennich, H.; Boman, H. Insect immunity. Attacins, a family of antibacterial proteins from *Hyalophora cecropia*. *EMBO J.* **1983**, *2*, 571–576. [[CrossRef](#)] [[PubMed](#)]
57. Bang, K.; Park, S.; Yoo, J.Y.; Cho, S. Characterization and expression of attacin, an antibacterial protein-encoding gene, from the beet armyworm, *Spodoptera exigua* (Hübner) (Insecta: Lepidoptera: Noctuidae). *Mol. Biol. Rep.* **2012**, *39*, 5151–5159. [[CrossRef](#)] [[PubMed](#)]
58. Yi, H.-Y.; Chowdhury, M.; Huang, Y.-D.; Yu, X.-Q. Insect antimicrobial peptides and their applications. *Appl. Microbiol. Biotechnol.* **2014**, *98*, 5807–5822. [[CrossRef](#)] [[PubMed](#)]
59. Hoffmann, J.A. Innate immunity of insects. *Curr. Opin. Immunol.* **1995**, *7*, 4–10. [[CrossRef](#)] [[PubMed](#)]
60. Eisenreich, W.; Heesemann, J.; Rudel, T.; Goebel, W. Metabolic host responses to infection by intracellular bacterial pathogens. *Front. Cell. Infect. Microbiol.* **2013**, *3*, 24. [[CrossRef](#)] [[PubMed](#)]
61. Galenza, A.; Foley, E. Immunometabolism: Insights from the *Drosophila* model. *Dev. Comp. Immunol.* **2019**, *94*, 22–34. [[CrossRef](#)]
62. Nunes, C.; Sucena, É.; Koyama, T. Endocrine regulation of immunity in insects. *FEBS J.* **2021**, *288*, 3928–3947. [[CrossRef](#)]
63. Sousa, A.P.; Cunha, D.M.; Franco, C.; Teixeira, C.; Gojon, F.; Baylina, P.; Fernandes, R. Which role plays 2-hydroxybutyric acid on insulin resistance? *Metabolites* **2021**, *11*, 835. [[CrossRef](#)]
64. Li, B.; Hong, Y.; Gu, Y.; Ye, S.; Hu, K.; Yao, J.; Ding, K.; Zhao, A.; Jia, W.; Li, H. Functional metabolomics reveals that astragalus polysaccharides improve lipids metabolism through microbial metabolite 2-hydroxybutyric acid in obese mice. *Engineering* **2022**, *9*, 111–122. [[CrossRef](#)]
65. Park, S.R.; Park, J.W.; Ban, Y.H.; Sohng, J.K.; Yoon, Y.J. 2-Deoxystreptamine-containing aminoglycoside antibiotics: Recent advances in the characterization and manipulation of their biosynthetic pathways. *Nat. Prod. Rep.* **2013**, *30*, 11–20. [[CrossRef](#)]
66. Li, S.; Sun, Y. Research advances in aminoglycoside biosynthesis. *Chin. J. Antibiot.* **2019**, *44*, 1261–1274.
67. Bendia, E.; Benedetti, A.; Baroni, G.S.; Candelaresi, C.; Macarri, G.; Trozzi, L.; Di Sario, A. Effect of cyanidin 3-O- β -glucopyranoside on hepatic stellate cell proliferation and collagen synthesis induced by oxidative stress. *Dig. Liver Dis.* **2005**, *37*, 342–348. [[CrossRef](#)]
68. Serafino, A.; Sinibaldi Vallebona, P.; Lazzarino, G.; Tavazzi, B.; Rasi, G.; Pierimarchi, P.; Andreola, F.; Moroni, G.; Galvano, G.; Galvano, F. Differentiation of human melanoma cells induced by cyanidin-3-O- β -glucopyranoside. *FASEB J.* **2004**, *18*, 1940–1942. [[CrossRef](#)]
69. Burnham, W.S.; Sidwell, R.W.; Tolman, R.L.; Stout, M.G. Synthesis and antiviral activity of 4'-hydroxy-5,6,7,8-tetramethoxyflavone. *J. Med. Chem.* **1972**, *15*, 1075–1076. [[CrossRef](#)] [[PubMed](#)]
70. Zhang, J.; Chen, Y.; Wang, M.; Zhong, L.; Li, L.; Yuan, Z.; Zou, S. Amino acid metabolism dysregulation associated with inflammation and insulin resistance in HIV-infected individuals with metabolic disorders. *Amino Acids* **2023**, *55*, 1545–1555. [[CrossRef](#)] [[PubMed](#)]
71. Sohn, J.H.; Mutlu, B.; Latorre-Muro, P.; Liang, J.; Bennett, C.F.; Sharabi, K.; Kantorovich, N.; Jedrychowski, M.; Gygi, S.P.; Banks, A.S. Liver mitochondrial cristae organizing protein MIC19 promotes energy expenditure and pedestrian locomotion by altering nucleotide metabolism. *Cell Metab.* **2023**, *35*, 1356–1372.e5. [[CrossRef](#)]
72. Freitag, D.; Ots, I.; Vanatoa, A.; Hörak, P. Immune response is energetically costly in white cabbage butterfly pupae. *Proc. R. Soc. London. Ser. B Biol. Sci.* **2003**, *270*, S220–S222. [[CrossRef](#)]
73. Dolezal, T.; Krejčova, G.; Bajgar, A.; Nedbalova, P.; Strasser, P. Molecular regulations of metabolism during immune response in insects. *Insect Biochem. Mol. Biol.* **2019**, *109*, 31–42. [[CrossRef](#)] [[PubMed](#)]
74. Arnold, P.A.; Johnson, K.N.; White, C.R. Physiological and metabolic consequences of viral infection in *Drosophila melanogaster*. *J. Exp. Biol.* **2013**, *216*, 3350–3357. [[CrossRef](#)]
75. Chambers, M.C.; Song, K.H.; Schneider, D.S. *Listeria monocytogenes* infection causes metabolic shifts in *Drosophila melanogaster*. *PLoS ONE* **2012**, *7*, e50679. [[CrossRef](#)] [[PubMed](#)]
76. Ardia, D.R.; Gantz, J.E.; Schneider, S. Costs of immunity in insects: An induced immune response increases metabolic rate and decreases antimicrobial activity. *Funct. Ecol.* **2012**, *26*, 732–739. [[CrossRef](#)]
77. Okamoto, N.; Yamanaka, N. Transporter-mediated ecdysteroid trafficking across cell membranes: A novel target for insect growth regulators. *J. Pestic. Sci.* **2021**, *46*, 23–28. [[CrossRef](#)] [[PubMed](#)]
78. Linton, K.J. Structure and function of ABC transporters. *Physiology* **2007**, *22*, 122–130. [[CrossRef](#)]
79. Pennacchio, F.; Caccia, S.; Digilio, M.C. Host regulation and nutritional exploitation by parasitic wasps. *Curr. Opin. Insect Sci.* **2014**, *6*, 74–79. [[CrossRef](#)] [[PubMed](#)]

80. Mrinalini; Siebert, A.L.; Wright, J.; Martinson, E.; Wheeler, D.; Werren, J.H. Parasitoid venom induces metabolic cascades in fly hosts. *Metabolomics* **2015**, *11*, 350–366. [[CrossRef](#)] [[PubMed](#)]
81. Tillinger, N.A.; Hoch, G.; Schopf, A. Effects of parasitoid associated factors of the endoparasitoid *Glyptapanteles liparidis* (Hymenoptera: Braconidae). *Eur. J. Entomol.* **2004**, *101*, 243–250. [[CrossRef](#)]
82. Liu, S.; Zhang, J.; Sheng, Y.; Feng, T.; Shi, W.; Lu, Y.; Guan, X.; Chen, X.; Huang, J.; Chen, J. Metabolomics provides new insights into host manipulation strategies by *Asobara japonica* (Hymenoptera: Braconidae), a fruit fly parasitoid. *Metabolites* **2023**, *13*, 336. [[CrossRef](#)]

Disclaimer/Publisher’s Note: The statements, opinions and data contained in all publications are solely those of the individual author(s) and contributor(s) and not of MDPI and/or the editor(s). MDPI and/or the editor(s) disclaim responsibility for any injury to people or property resulting from any ideas, methods, instructions or products referred to in the content.